Chemical Science

ROYAL SOCIETY OF CHEMISTRY

EDGE ARTICLE

View Article Online
View Journal

Check for updates

Cite this: DOI: 10.1039/d5sc07994b

All publication charges for this article have been paid for by the Royal Society of Chemistry

Received 16th October 2025
Accepted 7th December 2025

DOI: 10.1039/d5sc07994b

rsc.li/chemical-science

Open Access Article. Published on 24 December 2025. Downloaded on 12/24/2025 9:10:30 PM. This article is licensed under a Creative Commons Attribution 3.0 Unported Licence.

Unusual nitrene reactivity: imine formation in the photochemical reaction of a borylnitrene with ethene

Virinder Bhagat and Holger F. Bettinger *

The cycloaddition of nitrenes with olefins is an important method for the synthesis of aziridines. We report here that the reaction of catecholato borylnitrene CatBN with ethene upon long wavelength photoirradiation (λ > 550 nm) gives not only the expected aziridine, but also the imine CatBN=CHCH$_3$ under cryogenic matrix isolation conditions in solid neon at 4 K. Computational analysis reveals that the photochemically generated singlet CatBN ($^1A_1$ electronic state) can react with ethene to form the aziridine and a singlet 1,3-diradical intermediate. The latter arises from multi-state reactivity involving the nearly degenerate $^1A_1$ and $^1A_2$ nitrene singlet states. The singlet 1,3-diradical has a very low barrier for 1,2-H migration to give the imine. The observation of an imine in the reaction with an alkene reveals chemodivergence by highlighting a previously unobserved reactivity pathway in nitrene chemistry.

Introduction

The reaction of nitrenoids and free nitrenes with carbon–carbon double bonds is an important method for producing aziridines in organic synthesis.[1–10] The hallmark of singlet nitrenes R–N, electron deficient nitrogen species with an electron sextet, is their stereospecific cycloaddition reaction with olefins to yield aziridines.[2] The cycloaddition of singlet nitrenes with alkenes is a concerted reaction that preserves the stereochemistry of the alkene substituents (Scheme 1). In contrast, triplet nitrenes react in a stepwise fashion involving a triplet 1,3-diradical intermediate. As the rate of intersystem crossing to the lower energy singlet 1,3-diradical can be competitive with the rate of rotation about the C–C bond of the diradical, triplet nitrenes show only low or even no stereoselectivity in aziridine formation.[2]

In the gas phase reaction of imidogen NH and ethene, the primary products, aziridine and triplet 1,3-diradical, are formed in a vibrationally hot state and fragment to the ultimate stable products CH_3CN and HCN (Scheme 1, bottom).[11–14] Vibrationally excited aziridine is assumed to be in dynamic equilibrium with the singlet 1,3-diradical that can readily rearrange to an imine by 1,2-hydrogen shift.[13,15] The imine is assumed to be an intermediate of gas phase product formation, but has been rarely observed in the reaction of nitrenes with olefins.[8]

We here report detection of an imine in the reaction of a singlet borylnitrene with ethene. Borylnitrenes are a rather unusual class of nitrenes. The catecholato borylnitrene CatBN **1**, a triplet ground state species ($^3A_2$ electronic state) that can be observed using matrix isolation methods,[16] reacts upon very mild annealing with dioxygen O_2 to form nitritoborane CatBONO revealing that $^3A_2$-**1** is much more reactive than typical organic nitrenes.[16,17] Upon long wavelength irradiation (>550 nm), matrix isolated $^3A_2$-**1** forms $^1A_1$-**1** as supported by computational analysis of the excited state potential energy surfaces.[18] The highly electrophilic vinylidene-like $^1A_1$-**1** readily activates unreactive small closed-shell molecules by addition (N_2, CO, and CO_2) or insertion (CH_4 and H_2) into single bonds (Scheme 2a).[16,19–23] The triplet state of **1** does not react with these

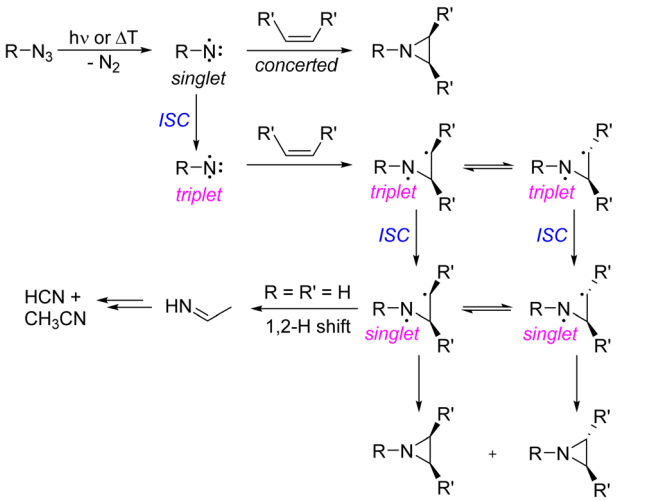

Scheme 1 Simplified reaction scheme of photochemically or thermally generated nitrenes with olefins. Aziridines are typically observed in solution, while in the gas phase fragmentation occurs in the reaction of triplet NH with ethene (R=R'=H).

Institut für Organische Chemie, Universität Tübingen, Auf der Morgenstelle 18, 72076 Tübingen, Germany. E-mail: holger.bettinger@uni-tuebingen.de

© 2025 The Author(s). Published by the Royal Society of Chemistry

Open Access Article. Published on 24 December 2025. Downloaded on 12/24/2025 9:10:30 PM.
This article is licensed under a Creative Commons Attribution 3.0 Unported Licence.

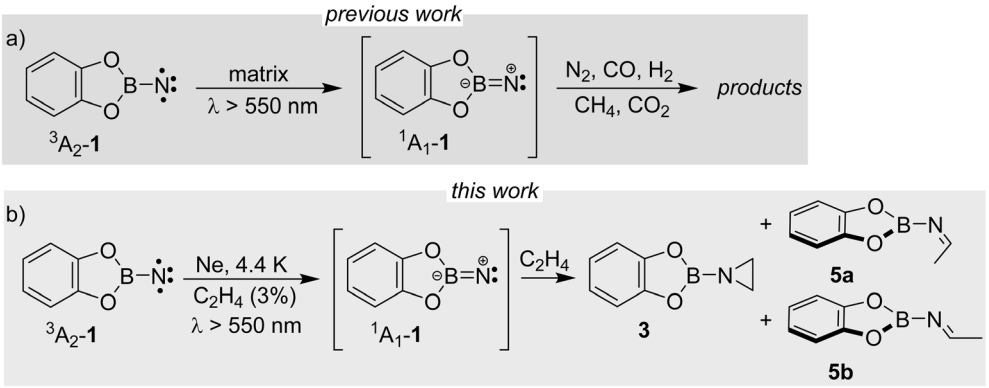

Scheme 2 (a) Photochemical reaction of triplet borylnitrene **1** with the closed-shell molecules; (b) products observed after photolysis of $^3A_2$-**1** to $^1A_1$-**1** in the presence of ethene under matrix isolation conditions.

unreactive species. In solution or the gas phase, borylnitrenes of the 1,3,2-dioxaborolane type insert into unactivated CH bonds allowing for amination of unusual substrates, such as cycloalkanes, methane, and tetramethylsilane presumably *via* the transient singlet nitrene.[19,21,24]

By combining matrix isolation IR spectroscopy and computational methods, we provide evidence that the reaction of CatBN with ethene yields, along with the expected aziridine, the isomeric imine, demonstrating chemodivergence[25] in this simple system (Scheme 2b). The imine likely results from the singlet 1,3-diradical, which in turn arises from the multi-state reactivity of the borylnitrene.

Results and discussion

To study the reaction of borylnitrene **1** with ethene C_2H_4, the borylazide $CatBN_3$ **2** was deposited with a large excess of neon gas doped with 3% C_2H_4 onto a cold CsI window maintained at 4 K. Thereafter, the deposited matrix was irradiated with light of wavelength $\lambda = 254$ nm, which resulted in the formation of borylnitrene **1** in its triplet ground state $^3A_2$ (Fig. S1a). The infrared (IR) signals assigned to **1** showed a shift compared to the reported IR data,[16] which is probably due to the complexation[26] to the dopant C_2H_4. In fact, we have experimental evidence supporting the observation of a complex between **1** and ethene (Fig. S2). Especially, the B–N/B–O wagging mode of the complex between **1** and ethene ($^3A_2$-**1**·C_2H_4) show a prominent red shift of 17 cm^{-1} compared to bare $^3A_2$-**1**, which matches exactly with the corresponding computed shift. In addition to the signals due to $^3A_2$-**1**, weak signals at 1760, 1742, 1520, 1506, and 1307 cm^{-1} were also observed. Subsequently, the matrix was irradiated with $\lambda > 550$ nm, as performed in our previous studies,[16,19,20,23] to populate the $^1A_1$ state of **1** that undergoes intermolecular reaction with C_2H_4.[18] The resulting

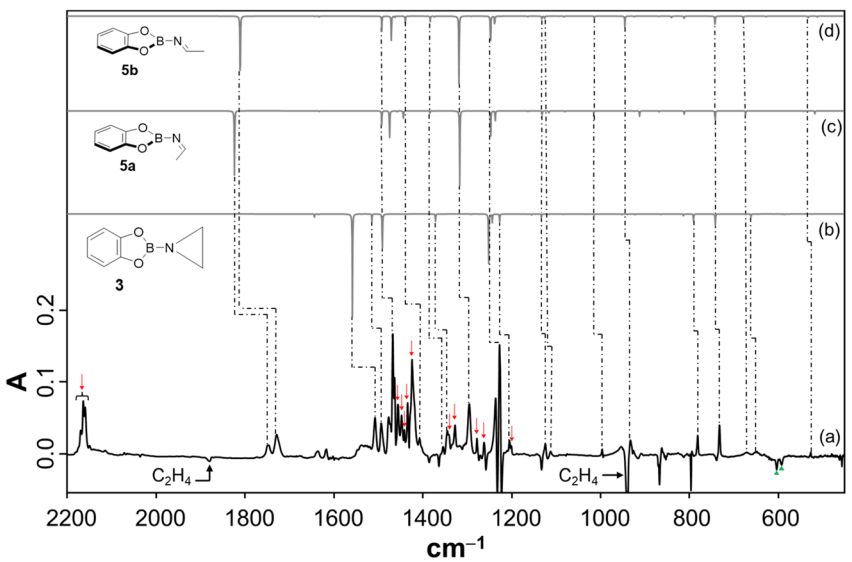

Fig. 1 (a) Difference spectrum after irradiating the Ne matrix with $\lambda > 550$ nm doped with 3% C_2H_4 for 120 min; (b–d) harmonic vibrational spectrum (unscaled) for the ^{11}B isotopologues of **3**, **5a**, and **5b**, respectively, calculated at the B3LYP/6-311+G(d,p) level of theory; (↓) corresponds to the IR bands of **2**, ▲ corresponds to the IR bands (see Fig. S2) of $^3A_2$-**1** that show a red shift upon complexation to ethene. Prior to this irradiation, the azide was decomposed to nitrene **1** and N_2 using $\lambda = 254$ nm.

© 2025 The Author(s). Published by the Royal Society of Chemistry

Open Access Article. Published on 24 December 2025. Downloaded on 12/24/2025 9:10:30 PM.
This article is licensed under a Creative Commons Attribution 3.0 Unported Licence.

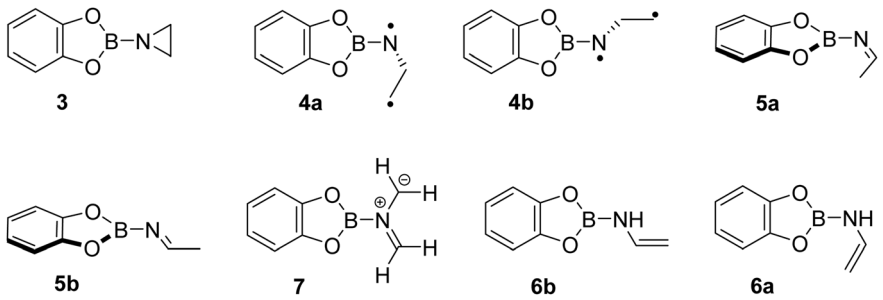

Chart 1 Potential products of the photoreaction between borylnitrene $^3A_2$-**1** and ethene.

difference spectrum illustrated in Fig. 1a shows the formation of azide **2** that we observed previously under these conditions,[16,19–23] the bleaching of IR bands related to C_2H_4, and the appearance of many additional IR bands at 1760, 1742, 1520, 1506, 1480, 1475, 1462, 1456, 1419, 1366, 1357, 1307, 1240, 1217, 1137, 1124, 1008, 944, 794, 744, 684, 660, and 539 cm^{-1}. The number of new IR bands indicates the formation of more than one species from the photoinduced reaction between $^1A_1$-**1** and ethene. There are a number of potential reaction products of this reaction, including aziridine **3**, diastereoisomeric imines **5a** and **5b**, conformational isomeric enamines **6a** and **6b**, and azomethine ylide **7** (Chart 1).[27–29]

Based on the computed spectra of these species (Fig. S3), the formation of isomeric enamines **6a** and **6b**, as well as azomethine ylide **7**, can safely be excluded. On the other hand, we surmised the formation of aziridine **3** and imine isomers, based on the IR bands positioned between 1700 and 1800 cm^{-1}. To further support the formation of these products, a comparison was made between the experimental difference spectrum resulting from $\lambda > 550$ nm irradiation and the computed IR spectra of **3**, **5a**, and **5b**, as shown in Fig. 1. The IR bands, such as 1520 and 1217 cm^{-1}, are composed of three-membered ring breathing modes and the one at 1506 cm^{-1} is composed of 3-membered ring CH_2 scissor motion, which are the signature IR bands of three-membered ring compounds.[30] Additionally, the band at 794 cm^{-1} is predominantly described by the characteristic C–C stretch of the terminal three-membered ring. In the 1800–1700 cm^{-1} region, strong IR bands signify the N=C stretching, while bands at 1307 cm^{-1} and 1366 cm^{-1} are due to the B–N=C–H scissor mode and symmetric bend of the terminal CH_3 groups, respectively, of **5a** and **5b**. These IR features are indicative of compounds containing the imine functional group.[31]

To further support the spectral assignments, the reaction between **1** and the $^{13}C_2H_4$ isotopologue of ethene was studied. The difference spectra resulting from $\lambda > 550$ nm irradiation (Fig. 2) show that the characteristic ring breathing modes are red shifted by 7 and 15 cm^{-1}, respectively. The CH_2 scissor

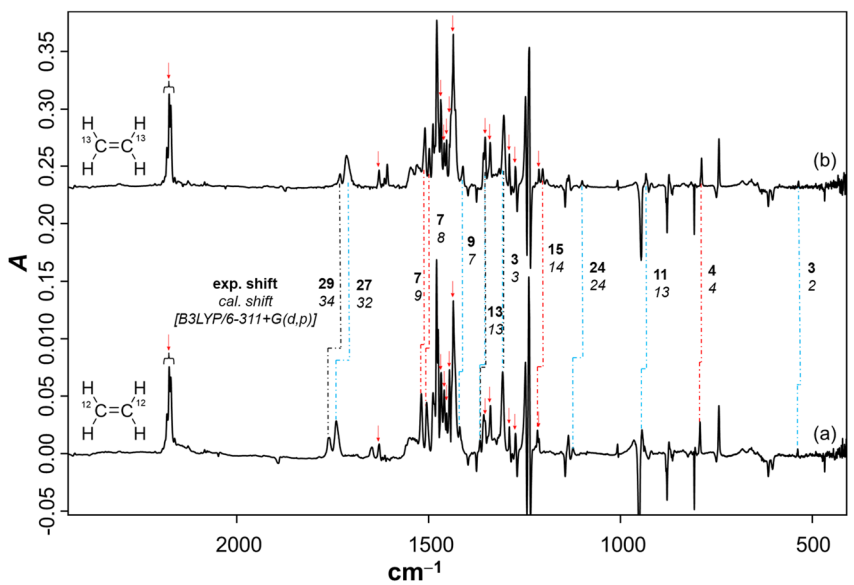

Fig. 2 (a) Difference spectrum after irradiating the Ne matrix with $\lambda > 550$ nm doped with 3% C_2H_4 for 120 min; (b) difference spectrum after irradiating the Ne matrix with $\lambda > 550$ nm doped with 3% $^{13}C_2H_4$ for 120 min; (↓) corresponds to the IR bands of **2**. (– · – · –), (– – – –), and (– · · – · · –) correspond to the experimental isotopic IR band shifts of **3**, **5a**, and **5b**. Prior to this irradiation, the azide was decomposed to nitrene **1** and N_2 using $\lambda = 254$ nm.

© 2025 The Author(s). Published by the Royal Society of Chemistry

Open Access Article. Published on 24 December 2025 9:10:30 PM. This article is licensed under a Creative Commons Attribution 3.0 Unported Licence.

mode and the characteristic C–C stretching mode of the terminal three-membered ring are red shifted by 7 cm^{-1} and 4 cm^{-1}, respectively. The experimental isotopic shifts match well with the corresponding computed isotopic shifts (Fig. 2). Similarly, the N=C stretches in **5a** and **5b** show isotopic red shifts of 29 and 27 cm^{-1}, which match well with the corresponding computed shifts of 34 and 32 cm^{-1}, respectively. Also, the common IR modes in the isomeric imines, CH_3 symmetric bend and B–N=C–H scissor, show isotopic red shifts of 13 and 3 cm^{-1}, respectively, which have a perfect match with the computed shifts. Moreover, the assignment of the products was further corroborated by performing the reaction of $^3A_2$-**1** with C_2D_4 (Fig. S4). In addition, the species from the previous step was tested under photoirradiation with $\lambda = 254$ nm, showing that aziridine **3** remains largely intact while **5b** photoisomerizes to **5a** (Fig. S10).

The unexpected formation of isomeric imines necessitated further computational investigation to understand the reaction mechanism. Previously, we have obtained computational evidence that the irradiation of **1** in its triplet ground state with $\lambda > 550$ nm populates the $^1A_1$ state.[18] Therefore, we consider the $^1A_1$ state as the starting point of our computational investigations that comprise two components: (1) the formation of primary products resulting from the reaction between $^1A_1$-**1** and ethene, and (2) the subsequent formation of secondary products. First, we studied the formation of the primary product aziridine **3** *via* a relaxed potential energy surface (PES) scan. The scan parameters r_1 and r_2, as shown in Fig. 3a, were constrained

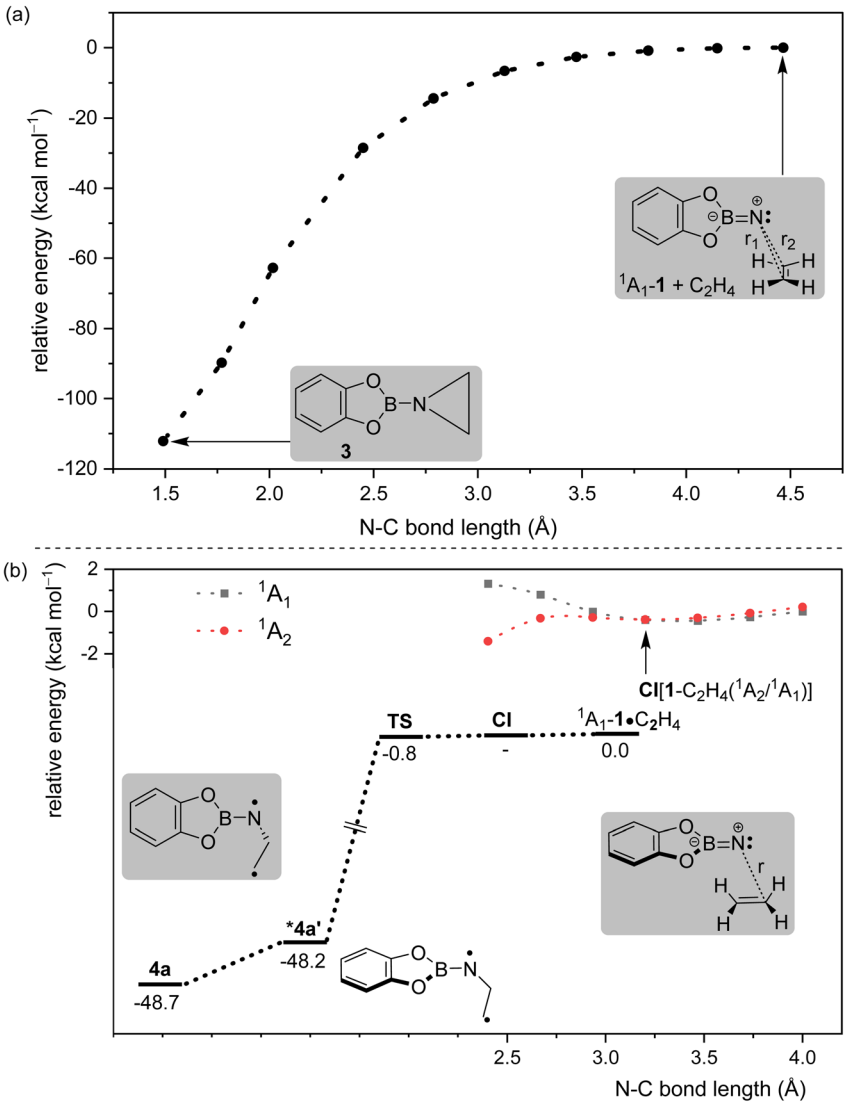

Fig. 3 (a) Relaxed potential energy surface scan with constrained bond distances, r_1 and r_2 ($r_1 = r_2$), between the nitrogen atom of $^1A_1$-**1** and both carbon atoms of ethene calculated at the B2PLYPD3/def2-TZVPP level of theory; (b) lower half: potential energy surface leading to the formation of *syn*-1,3-diradical **4a** starting from the complex $^1A_1$-**1**·C_2H_4 calculated at the CASPT2/def2-TZVPP//CASPT2/def2-SV(P) level of theory; upper right corner: partial relaxed potential energy surface scan in a bisected manner (similar to $^1A_1$-**1**·C_2H_4) with a constrained bond distance *r* between the nitrogen atom of **1** and one of the carbon atoms of ethene, calculated at the CASPT2/def2-TZVPP//B2PLYPD3/def2-TZVPP level of theory (see the SI for details of the CASPT2 calculations). The conical intersection (CI) is marked by an arrow. * Second-order saddle point.

© 2025 The Author(s). Published by the Royal Society of Chemistry

Open Access Article. Published on 24 December 2025 9:10:30 PM. This article is licensed under a Creative Commons Attribution 3.0 Unported Licence.

to the same value at each step of the scan to ensure *quasi*-C_s symmetry throughout the process. The PES has no barrier for the formation of aziridine and therefore supports the experimental observation of **3**.

In addition, the reaction was studied with a different reaction coordinate, as shown in Fig. 3b, as the second part of the primary reaction. In this reaction, the planes containing **1** and ethene lie parallel to each other at the start of the reaction (pre-reactive complex). The pre-reactive complex is a good starting point considering the available experimental evidence for such a complex, as discussed above (Fig. S2). Considering the possibility of the multireference character of the wavefunctions of different species along this reaction coordinate, complete active space second-order perturbation (CASPT2) theory was chosen. The calculated stationary points show the barrierless formation of 1,3-diradical **4a** (Fig. 3b). A partial PES scan was performed with *r* as the scan parameter (Fig. 3b) to show the transfer of population from initially populated $^1A_1$ to the $^1A_2$ state of **1** along such a reaction coordinate through a conical intersection (CI).

The observation of imine products in the experimental studies could be explained by the second part of our computational studies. Herein, we have computed a PES starting from aziridine **3** and 1,3-diradical **4a**, as shown in Fig. 4 (highlighted in grey). Conversion of **3** into isomeric imines **5a** and **5b** can proceed *via* isomeric 1,3-diradicals **4a** and **4b**, respectively. Since these steps involve high energy barriers of around 57–59 kcal mol^{-1}, these paths are not feasible for the formation of

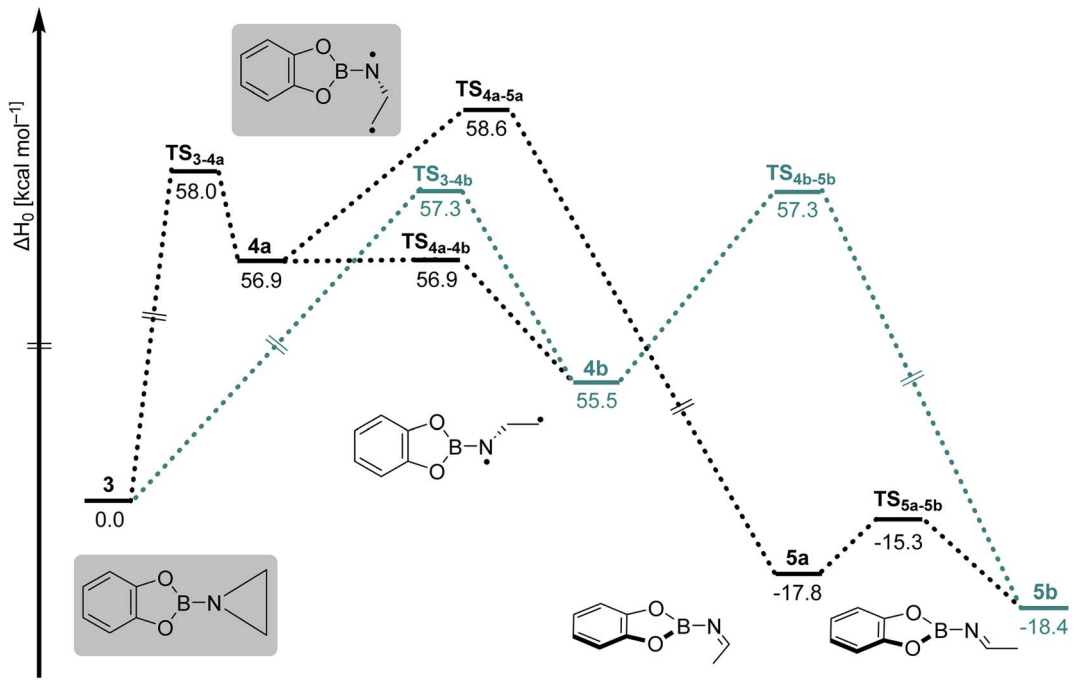

Fig. 4 Potential energy surface initiating from aziridine **3** and *syn*-1,3-diradical **4a** calculated at the B2PLYPD3/def2-TZVPP level of theory.

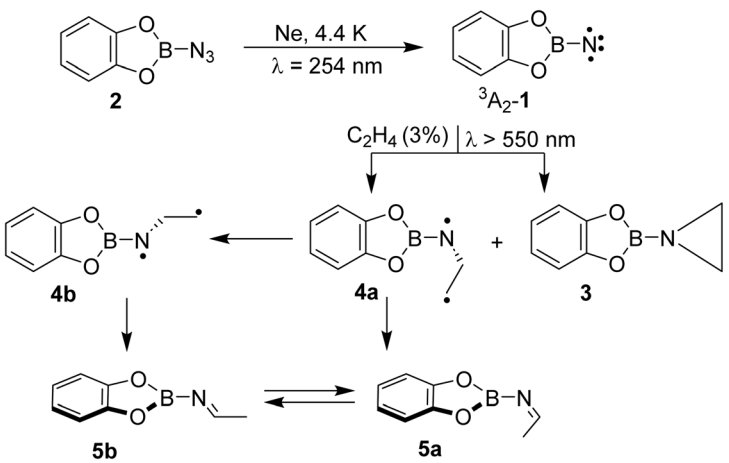

Scheme 3 Formation of aziridine **3** and isomeric imines **5a** and **5b** resulting from the reaction of borylnitrene **1** and ethene.

Open Access Article. Published on 24 December 2025. Downloaded on 12/24/2025 9:10:30 PM. This article is licensed under a Creative Commons Attribution 3.0 Unported Licence.

isomeric imines under the cryogenic conditions employed in our experiments if energy transfer to the surrounding matrix is efficient. Furthermore, IR measurements of the ^{13}C-labeled reaction (Fig. S11) at various time intervals reveal the formation of **5a**/**5b** without accumulation of **3**, suggesting that the imines form independently rather than as secondary photoproducts. On the other hand, the formation of **5a** *via* a 1,2-H shift to the terminal carbon atom of **4a** has a barrier of merely 1.7 kcal mol^{-1}, which can be surpassed in cryogenic matrices at 4 K. In addition, the conversion of **4a** into **4b** has a negligible barrier, which in turn has an accessible energy barrier of 1.8 kcal mol^{-1} for its conversion into **5b**. Furthermore, starting from **4a** and **4b**, we explored the possibility of forming enamine products **6a** and **6b** through a 1,2-H shift to the nitrogen atom, as shown in Fig. S5. High barriers for the formation of isomeric enamines from **4a** and **4b**, compared to the isomeric imines, support their experimental absence.

Conclusions

The combined matrix isolation and computational studies regarding the photochemical reactivity of **1** with ethene demonstrate the formation of aziridine **3** and isomeric imines **5a** and **5b**, as shown in Scheme 3. Notably, the formation of isomeric imines is rare for such a reaction. Computational studies support the formation of singlet 1,3-diradical **4a**, which could not be observed experimentally, as an alternate primary product alongside the expected aziridine **3**. Finally, the diradical **4a** has accessible energy barriers for its conversion into imines **5a** and **5b**. The observations are remarkable as the formation of the 1,3-diradical intermediate in cycloaddition reactions of nitrenes is the hallmark of triplet state reactivity, while here the singlet state is involved. The low barrier for collapse of the diradical to the imines **5** and aziridine **3** suggests that these processes are very fast. We are currently investigating the dual mode reactions of borylnitrenes with olefins in solution to shed more light onto this unusual reactivity.

Author contributions

V. B. conducted all calculations, experiments involving matrix isolation, and data analysis. V. B. and H. F. B. jointly wrote the first draft of the manuscript. H. F. B. conceived the research idea, revised the manuscript, and secured funding.

Conflicts of interest

The authors declare no competing interests.

Data availability

The data that support the findings of this study are available in the supplementary information (SI) of this article. Supplementary information: matrix isolation spectra, peak tables, computational details, and Cartesian coordinates. See DOI: https://doi.org/10.1039/d5sc07994b.

Acknowledgements

The authors thank the German Research Foundation (DFG) for support of this work through project 460087109. The computations were performed on the BwForCluster JUSTUS2 cluster. The author acknowledges support by the state of Baden-Württemberg through bwHPC and the DFG through grant no. INST 40/575-1 FUGG (JUSTUS 2 cluster) for computation facilities.

References

1 K. Lee, K. Seo, M. Dehghany, Y. Hu, A. Trinh and J. M. Schomaker, in *Heterocycles from Carbenes and Nitrenes : Methods, Reactions and Synthetic Applications*, ed. M. P. Doyle and X. Xu, Springer International Publishing, Cham, 2023, pp. 313–377.
2 W. Lwowski, *Angew Chem. Int. Ed. Engl.*, 1967, **6**, 897–906.
3 N. Baris, M. Dračínský, L. J. Tóth, B. Klepetářová and P. Beier, *Org. Chem. Front.*, 2025, **12**, 5610–5615.
4 N. Baris, M. Dračínský, J. Tarábek, J. Filgas, P. Slavíček, L. Ludvíková, S. Boháčová, T. Slanina, B. Klepetářová and P. Beier, *Angew. Chem., Int. Ed.*, 2024, **63**, e202315162.
5 Y.-A. Xu, S.-H. Xiang, J.-T. Che, Y.-B. Wang and B. Tan, *Chin. J. Chem.*, 2024, **42**, 2656–2667.
6 A. R. Meyer, M. V. Popescu, A. Sau, N. H. Damrauer, R. S. Paton and T. P. Yoon, *ACS Catal.*, 2024, **14**, 12310–12317.
7 M. S. Platz, in *Reactive Intermediate Chemistry*, 2003, pp. 501–559.
8 S. O. Scholz, E. P. Farney, S. Kim, D. M. Bates and T. P. Yoon, *Angew. Chem., Int. Ed.*, 2016, **55**, 2239–2242.
9 M. Holzinger, J. Abraham, P. Whelan, R. Graupner, L. Ley, F. Hennrich, M. Kappes and A. Hirsch, *J. Am. Chem. Soc.*, 2003, **125**, 8566–8580.
10 M. Holzinger, O. Vostrowsky, A. Hirsch, F. Hennrich, M. Kappes, R. Weiss and F. Jellen, *Angew. Chem., Int. Ed.*, 2001, **40**, 4002–4005.
11 D. W. Cornell, R. S. Berry and W. Lwowski, *J. Am. Chem. Soc.*, 1966, **88**, 544–550.
12 S. P. Devi, T. Salam and R. H. Duncan Lyngdoh, *J. Chem. Sci.*, 2016, **128**, 681–693.
13 B. Du, W. Zhang, L. Mu and C. Feng, *J. Mol. Struct.: THEOCHEM*, 2007, **816**, 21–29.
14 M. Röhrig and H. G. Wagner, *Ber. Bunsenges. Phys. Chem.*, 1994, **98**, 864–868.
15 T. Fueno, K. Yamaguchi and O. Kondo, *Bull. Chem. Soc. Jpn.*, 2006, **63**, 901–912.
16 H. F. Bettinger and H. Bornemann, *J. Am. Chem. Soc.*, 2006, **128**, 11128–11134.
17 V. Bhagat, J. Schumann and H. F. Bettinger, *Chem.–Eur. J.*, 2020, **26**, 12654–12663.
18 V. Bhagat and H. F. Bettinger, *J. Phys. Chem. A*, 2022, **126**, 7660–7666.
19 H. F. Bettinger, M. Filthaus, H. Bornemann and I. M. Oppel, *Angew. Chem., Int. Ed.*, 2008, **47**, 4744–4747.
20 H. F. Bettinger, M. Filthaus and P. Neuhaus, *Chem. Commun.*, 2009, 2186–2188.

© 2025 The Author(s). Published by the Royal Society of Chemistry

Open Access Article. Published on 24 December 2025. Downloaded on 12/24/2025 9:10:30 PM.
This article is licensed under a Creative Commons Attribution 3.0 Unported Licence.

21 H. F. Bettinger and M. Filthaus, *Org. Biomol. Chem.*, 2010, **8**, 5477–5482.
22 H. F. Bettinger and H. Bornemann, *Z. Anorg. Allg. Chem.*, 2011, **637**, 2169–2174.
23 V. Bhagat, J. Schumann and H. F. Bettinger, *Angew. Chem., Int. Ed.*, 2021, **60**, 23112–23116.
24 M. Filthaus, L. Schwertmann, P. Neuhaus, R. W. Seidel, I. M. Oppel and H. F. Bettinger, *Organometallics*, 2012, **31**, 3894–3903.
25 I. P. Beletskaya, C. Nájera and M. Yus, *Chem. Soc. Rev.*, 2020, **49**, 7101–7166.
26 Y. Du, X. Li, J. Jiang, W. Fan, D. Mu, Q. Li, R. Ma, Q. Yu and X. Zeng, *J. Phys. Chem. Lett.*, 2025, **16**, 7127–7133.
27 A. V. Kuzmin and B. A. Shainyan, *J. Phys. Org. Chem.*, 2014, **27**, 794–802.
28 T. Fueno, V. Bonacic-Koutecky and J. Koutecky, *J. Am. Chem. Soc.*, 1983, **105**, 5547–5557.
29 E. Jacox and D. E. Milligan, *J. Am. Chem. Soc.*, 1963, **85**, 278–282.
30 G. Herzberg, *Infra-Red and Raman Spectra of Polyatomic Molecules*, D. Van Nostrand Co., Inc., New York, 1945.
31 A. Melli, M. Melosso, N. Tasinato, G. Bosi, L. Spada, J. Bloino, M. Mendolicchio, L. Dore, V. Barone and C. Puzzarini, *Astrophys. J.*, 2018, **855**, 123.